J Solid State Electrochem (2010) 14:599–613
DOI 10.1007/s10008-009-0819-0

ORIGINAL PAPER

Composite electrodes consisting Pt nano-particles and poly (aminophenols) film on pre-treated aluminum substrate as electrocatalysts for methanol oxidation

Biuck Habibi · Mohammad Hossien Pournaghi-Azar

Received: 11 October 2008 / Revised: 12 January 2009 / Accepted: 26 February 2009 / Published online: 17 March 2009

Abstract Electrochemically platinum plated aluminum (Al/Pt) was used as an electrode substrate for the electropolymerization of aminophenols and fabrication of composite electrodes based on platinum nano-particles. The poly(*o*-aminophenol) (P*o*AP), poly(*m*-aminophenol) (P*m*AP), and poly(*p*-aminophenol) (P*p*AP) were synthesized on the Al/Pt electrode, and further modification was performed by deposition of platinum nano-particles onto polymer matrixes. The electrochemical and morphological characteristic of the composed electrodes were carried out by cyclic voltammetry and scanning electron microscopy, respectively. The electrocatalytic oxidation of methanol on the composite electrodes was studied by cyclic voltammetry in 0.1 M sulfuric acid as supporting electrolyte. It was found that the Al/Pt/P*o*AP electrode incorporated Pt nano-particles (Al/Pt/P*o*AP/Pt) exhibits a higher electrocatalytic activity for the oxidation of methanol than the Al/Pt/P*m*AP/Pt and Al/Pt/P*p*AP/Pt electrodes. On the other hand, a higher catalytic current for methanol oxidation was found on the Al/Pt/P*o*AP/Pt electrode in comparison to bulk Pt and Al–Pt (Al with 0.2 mg cm^{-2} of Pt particles) electrodes. The effects of various parameters such as thickness of the polymer film, concentration of the monomer, Pt loading method and the Pt amounts, concentration of the methanol, and the medium temperature were studied on the electrooxidation of methanol. The long-term stability of the modified electrode has also been investigated.

Keywords Aluminum electrode · Poly(aminophenols) · Poly(*o*-aminophenol)–Pt composite electrode · Electrooxidation of methanol

B. Habibi (✉)
Electroanalytical Chemistry Laboratory, Faculty of Sciences,
Department of Chemistry,
Azarbaijan University of Tarbiat Moallem,
Tabriz, Iran
e-mail: B.Habibi@azaruniv.edu

M. H. Pournaghi-Azar
Electroanalytical Chemistry Laboratory, Faculty of Chemistry,
University of Tabriz,
Tabriz, Iran

Introduction

Studies aiming at developing efficient fuel cells have greatly contributed to the development of catalysts for the electrooxidation of small organic molecules. Among these substances, methanol has been the most investigated due to the possibility of using it as a fuel in direct methanol fuel cells (DMFC). It is largely accepted that Pt and Pt alloys are the best materials for the electrooxidation of methanol [1–5]. However, the increasing use of Pt and Pt alloys may raise the price of electrocatalyst and deplete a scarce resource.

Three possible approaches were tried to circumvent the problem of using these metals in DMFCs and related applications. In a straightforward approach, Pt- based electrocatalysts have been prepared by deposition of its particles on less expensive materials [6–13]. In another approach, bi- or tri-metallic catalysts involving transition metals were attempted [14–18]. In the last approach, some electrodes have been fabricated through incorporation of Pt and Pt alloys micro- or nano-particles into conducting polymer matrices [19–26]. The conducting polymers used are mainly polyaniline, polypyrrole, and polythiophene. These polymers offer great advantages due to their very good conducting, good mechanical properties, and good adhesion to the electrode substrate. However, it is of interest to extend such studies to other polymers [23, 27,

28], which might be suitable as host materials, especially on low price substrates, for the catalyst micro- and nano-particles. Aminophenols are interesting electrochemical materials since, differently from aniline [29] and other substituted anilines [30], they present two groups (NH_2 and OH), which could be oxidized. Therefore, they could show electrochemical behavior resembling anilines [31] or phenols [32]. These groups bonding up with the polymeric molecules can constitute reactive sites for incorporation of metals [33, 34] or biomolecules [35], with applications in electrocatalysis and electrochemical biosensors. Literature survey shows that the electropolymerization of aminophenols was studied on various substrates [36–41]. However, its electropolymerization on the aluminum electrode, which is a low-price substrate, has not been reported hitherto.

The goals of this study are (1) pre-treatment of the aluminum substrate by electroplating of the Al surface (Al/Pt) likes our previous works [25, 42] and subsequent electrodeposition of the stable poly(aminophenols) (PAPs) film on the Al/Pt electrode, (2) confining the Pt nano-particles by electrochemical deposition in PAPs matrixes (Al/Pt/PAPs/Pt), and (3) evaluation of the performance characteristics of the Al/Pt/PAPs/Pt electrodes as anodes for electrocatalytic oxidation of methanol.

Experimental

Chemicals

The aluminum bar with certified purity of 99.9% purchased from Tabriz Wire & Cable (Simcat, Iran) was used as substrate for the electrode matrix. H_2PtCl_6, sulfuric acid, *o*, *m* and *p*-aminophenol, methanol, and other chemicals were of analytical grades from Merck.

Procedures

Preparation of Al electrode

A cylindrical aluminum bar of 90 mm in length and 12 mm in diameter was used for the preparation of the aluminum disk electrode as follows:One the end of the Al bar was threaded by means of a suitable screw tap in order to connect it to an available holder or rotating disk system. From the other end of the bar, one part (30 mm in length) was ground until its diameter reached to 3 mm, then was fitted into a hole which was previously made in a Teflon rod of 12 mm in diameter and 30 mm in length [43]. The aluminum surface fitted in Teflon was mechanically polished successively to a mirror finish, first with 200, 600, 1,000, and 1,500 emery papers and then with 0.05 μm alumina powder. The polished surface was cleaned by dipping in concentrated HCl for about 1 min and rinsed with distilled water.

Fabrication of composite electrode

Fabrication of the composite electrode was performed in three steps:

1. Electroplating of the surface of Al disk electrode with Pt was performed by the electroreduction of H_2PtCl_6 (1 mM) in 0.5 M phosphate buffer solution using the potentiostatic method at constant potential of −0.60 V vs. SCE [12]. In this way, the amount of Pt deposited on the Al electrode has been controlled by the charge that passed during platinum electrodeposition under constant potential. Based on Faraday's law, this charge corresponds to ca. 12 mC cm^{-2}, i.e., 6 μg Pt cm^{-2} of Al electrode surface (assuming the 100% current efficiency by ignoring the simultaneous hydrogen evaluation in the present conditions).
2. Electropolymerization of aminophenols on the Al/Pt electrode was achieved by potentiodynamic method. The electrode potential was swept between −0.4 and 1.0 V at scan rate of 50 mV s^{-1} using an aqueous solution of 80 mM aminophenols and 0.1 M sulfuric acid as electrolyte. The thickness of the deposited films was controlled from the charge consumed during the formation of the aminophenols films. The overall anodic charge, Q_a, was integrated by PGSTAT-30 potentiostat/galvanostat. For a given Q_a, the thickness of deposited PAPs was estimated using Faraday law ($d_n=Q_aM/nF\rho$), considering a value of 2 for *n* and 109 for aminophenols molecular weight (*M*). Assuming a value of about 1.30 g cm^{-3} for PAPs density (ρ) at 20 °C (P*o*AP density at 20 °C is 1.283 g cm^{-3} [44]) and the geometric area of Al/Pt electrode as 0.07 cm^2, the PAPs film thickness (d_n) can easily be calculated [45]. A mean value of 0.6 μm was obtained for polymer film thickness when Q_a is ~140 mC cm^{-2}.
3. Platinum nano-particles were deposited onto polymers film by electrochemical deposition from an aqueous 0.1 M sulfuric acid solution of 1 mM H_2PtCl_6 using two different electrochemical techniques. Potentiostatic loading of platinum was performed by keeping the potential of the electrode at −0.2 V. In the potentiodynamic method, the loading of platinum was accomplished by electroreduction of H_2PtCl_6 (1 mM) in 0.1 M sulfuric acid, by sweeping the potential from −0.3 to +0.8 V with scan rate of 50 mV s^{-1}.

The quantity of electricity, Q_{dep}, mC cm^{-2}, resulting from the $PtCl_6^{2-}$ reduction is used for the evolution of loaded Pt. The Pt loading (W in mg cm^{-2}) is then

calculated:

$$W = Q_{\text{dep}} M / zF^{\sim} \quad (1)$$

Where M=195.078 g mol^{-1} is the atomic weight of Pt, z=4 is the number of exchanged electrons, and F=96,485.309 C mol^{-1} is the faradic constant.

However, due to charging of the conducting film and concurrent hydrogen evolution, the platinum loading level calculated by using this technique should be regarded as upper-value estimates. The loading of platinum in the present work was 0.2 mg cm^{-2}. For loading 0.2 mg cm^{-2} of Pt, the electrodeposition of Pt was performed by an electricity charge about of 400 mC cm^{-2}.

Determination of the active surface area of the Pt particles in composite electrodes was carried out by the evaluation of the quantity of electricity associated with the electrooxidation of CO previously adsorbed. The CO adsorption was carried out at −0.25 V vs. SCE by passing CO of high purity (99.95%) through a 0.1 M sulfuric acid aqueous solution for 5 min. With the electrode polarized at −0.25 V vs. SCE, the excess of CO in the solution was removed by bubbling nitrogen for 30 min. The stripping of CO was performed with scan rate of 5 mV s^{-1} in the potential range −0.25–1.10 V vs. SCE. The active area was calculated, assuming that a full monolayer of CO adsorbed on the electrode involves 420 μC cm^{-2}. The specific surface area S (in m^2 g^{-1}) was also estimated as follows:

$$S = 100 A_{\text{r}} / \left(W A_{\text{g}} \right) \quad (2)$$

with A_{r} is the real surface area, A_{g} is the geometric surface area (A_{g}=0.07 cm^2), and W (in μg cm^{-2}) is the platinum loading.

Assuming spherical particles of similar radius, a mean particle size of Pt, d (in nm), was calculated from the following equation using the procedure of Gloaguen et al. [7]:

$$d = 6,000 / (\rho S) \quad (3)$$

where ρ is the density of platinum (ρ =21.4 g cm^{-3}), and S is the specific surface area (in m^2 g^{-1}).

Instrumentation

The electrochemical experiments were carried out using an AUTOLAB PGSTAT-30 potentiostat/galvanostat connected to a personal computer through an USB electrochemical interface. A conventional three-electrode cell was used. The temperature of the cell was varied from 25 to 75 °C by circulation of thermostated water, using a heated water circulator (EYELA-DIGITAL UNI ACE UA-10). The working electrode was an Al/Pt/P*o*AP/Pt and Al/Pt/P*m*AP/Pt or Al/Pd/P*p*AP/Pt modified electrodes (with a diameter of 3 mm). A saturated calomel electrode and platinum wire were used as the reference and the auxiliary electrodes, respectively. The scanning electron microscopy (SEM) micrographs were obtained on a LEO 440i Oxford instrument.

Results and discussion

As the electrooxidation of methanol at the Al/Pt electrode covered by a thin film of PAPs incorporated platinum nanoparticles is the capital aim of this work, a brief study about the preparation and properties of Al/Pt/PAPs modified electrodes seems to be proper initially.

Electropolymerization of aminophenols on the Al/Pt electrode

The primary investigation showed that the electropolymerization of aminophenols at the surface of bare Al electrode achieved neither by potentiodynamic nor by potentiostatic methods similar to phenylenediamines [25] and aniline [42, 46]. To overcome this, initially the Al surface was treated electrochemically in an H_2PtCl_6 solution to obtain an Al/Pt electrode as described in "Experimental" section. Figure 1a shows the electropolymerization of *o*-aminophenol on the Al/Pt electrode by potentiodynamic method in an aqueous solution containing 0.1 M sulfuric acid and 80 mM monomer. As can be seen in Fig. 1a, in the first anodic sweep the oxidation of *o*AP occurs as a distinct irreversible broad anodic peak "*a*" (E_{p}=0.61 V) in the potential region 0.4–0.85 V, where P*o*AP has low conductivity, which decreases the monomer oxidation current. Part of the oxidation products of *o*AP is deposited on the electrode, i.e., the P*o*AP growth process, which is a ladder-conducting polymer with a phenoxazine-like chain structure [47], begins to take place.

In the first reverse cycle, the new cathodic peak at around −0.27 V appears (peak *b*′), confirming the initial deposition of electrooxidized products. In the second positive scan, there was an anodic peak at around −0.13 V (peak *b*). Along with the increase in the number of potentials cycles, the anodic peak current *a* decreased significantly, and potential of the peak shifted negatively from 0.61 to around 0.48 V. This decrease in oxidation current is due to the loss of activity of the electrode surface when covered with newly formed polymer film. The current of peaks *b*′ and *b* increases with increasing the number of potential cycles reflecting to coverage of the electrode surface by the polymeric film. With repetitive cycling, an increasingly thick, red color film is deposited on the Al/Pt electrode. Inset of Fig. 1a shows the usual images of Al/Pt and Al/Pt/P*o*AP film in two different thicknesses. On the

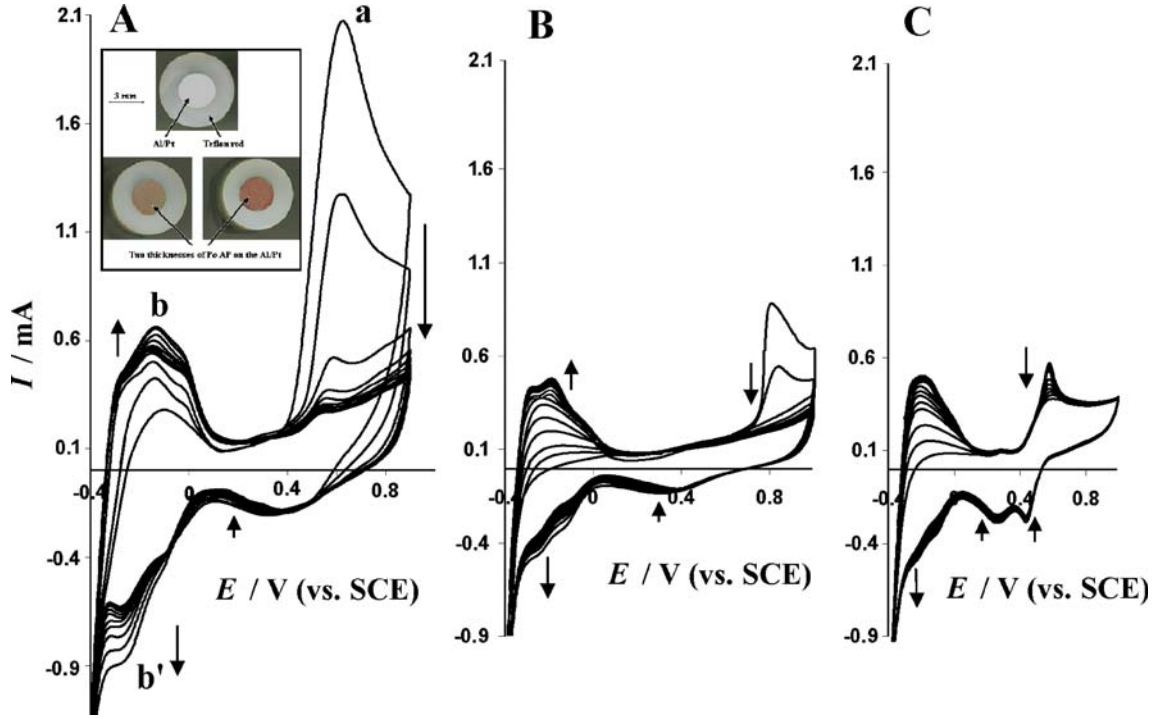

Fig. 1 Cyclic voltammograms (15 cycles) recorded during potentiodynamic growth of PAPs films on the Al/Pt electrode in solution containing 80 mM aminophenols and 0.1 M sulfuric acid at a scan rate of 50 mV s^{-1}. **a** P*o*AP, **b** P*m*AP, and **c** P*p*AP. *Inset* is the usual images of Al/Pt and Al/Pt/P*o*AP electrodes with two different thicknesses of P*o*AP film. Amount of Pt on the Al, 6 μg cm^{-2}

basis of visual investigation, the surface of the Al/Pt electrode is grayish as expected from Pt particles layer. On the other hand, as the thickness of PoAP film increases on the electrode surface, its red color became darker, and surface of electrode is covered completely.

The oxidation process of *o*AP is complex owing to the presence of two susceptible groups, –OH and $–NH_2$, and there is controversy in the literature with regard to dimeric structures formed after electrochemical oxidation of *o*AP in aqueous medium. From the results presented in the literature so far and taking account of the proposed mechanism for anodic oxidation of aniline in aqueous solutions [48], it is now generally accepted that the principal mechanism in electrochemical oxidation *o*AP and preparation of P*o*AP film [49, 50] is oxidation of *o*AP to cation radical (oAP^+), a "head-to-tail" coupling of two cation radicals leading the dimer aminodiphenylamine similar to the C–O–C coupling of phenols [51, 52] and finally formation of polymer involving structure **A** (phenoxazine units).

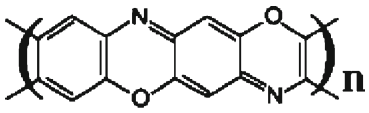

A

Similarly, Fig. 1b and c shows the electropolymerization of *m* and *p*-aminophenol on the Al/Pt electrode, respectively. As can be seen in Fig. 1b and c, the electropolymerization of *m*- and *p*-aminophenol proceeded as described for *o*-aminophenol. Only slight differences were observed in oxidation peak potential of monomers and redox peaks characteristics of the polymers.

The effect of the Pt amount on the pre-treated Al surface was investigated in the electropolymerization of aminophenols. For this purpose, the minimum amount of Pt required for formation only one flat layer of Pt was examined. Theoretically, according to $A=n \times \pi r^2$, the necessary numbers of Pt atoms (n) can be calculated, where r is the atomic radius of Pt, and A is the geometric surface area of the Al. Considering that r and A are 3 Å and 0.07 cm^2, respectively, and atomic mass of Pt is 195.078 g mol^{-1}, we calculated that 0.043 μg Pt (i.e., 0.61 μg cm^{-2} of Al surface) is necessary for formation of one flat Pt layer. According to Faraday's law, this value of Pt corresponds to charge density of 1.2 mC cm^{-2}. We have found that the electropolymerization of aminophenols did not occur for charge density of 1.2 mC cm^{-2}, whereas a compact layer of polymer is formed when the charge density for Pt deposition is reached to a suitable value of 12 mC cm^{-2}. This corresponds to deposition of 6 μg Pt cm^{-2} of Al electrode or about ten flat Pt layers (assuming the 100% current efficiency and a FCC crystal structure for the Pt deposit). It seems that such extraordinary charge density is not true for the electrode pretreatment by deposition of few layer of Pt, probably due to

the simultaneous hydrogen evaluation in the present conditions. However, we chose a charge density of 12 mC cm^{-2} as a required value during Al electrode plating.

Electrochemical and morphological characterization of the polymers

Once electropolymerization is accomplished, the polymer-coated electrode is removed from the cell and rinsed copiously with deionized water. The electrode is then characterized by cyclic voltammetry at a scan rate of 50 mV s^{-1} in an aqueous monomer free 0.1 M sulfuric acid solution. Figure 2 shows the cyclic voltammograms relating to the Al/Pt/modified with PAPs films (Al/Pt/PAPs) with optimum thickness. As can be seen in Fig. 2a, the P*o*AP has a large electroinactive region (bare region) above 0.1 V, similar to that observed on inert electrodes [52, 53] and a redox active range from −0.4 to 0.1 V. The oxidation and reduction currents in this region are attributed to the redox reaction in the polymer film, i.e., protonation and deprotonation of ladder-like and linear-chain polymer [54]. Similarly, Fig. 2b and c shows the cyclic voltammograms of P*m*AP and P*p*AP at Al/Pt electrode, respectively. As can be seen in Fig. 2b and c, the cyclic voltammograms of P*m*AP and P*p*AP have only slight differences with that of P*o*AP in the same conditions. Based on Ortega's study [53, 55], the electronic conductivity of poly *o*-aminophenol depends on the pH and electrode potential in aqueous solution. The conductivity of this polymer passes through a fairly narrow maximum in acidic solution. On the other hand, in the potentials region between −0.2 and 1.0 V vs. SCE, it is maximal at the formal potential of the polymer (defined as $(E_{pc}+E_{pa})/2$) [55]. It is also reported that the electrode coated with P*o*AP film responds to some dissolved organic neutral and/or inorganic species in potentials where it is non-conductive due to the perm-selective properties of the polymer [56]. Therefore, it was used repeatedly as a matrix for loading of metals particles for electrocatalysis proposes.

Figure 3 shows the surface morphology of the Al, Al/Pt, and PAPs films synthesized by potentiodynamic method on the Al/Pt electrodes. Figure 3a shows the structure of the bare aluminum surface immediately after polishing with emery paper grade 1500. As seen in this image, the surface is almost smooth and uniform without any holes or cavities. Figure 3b shows the surface of the same electrode after pre-treatment with Pt. Due to few platinum deposition, non-spherical platinum crystals were formed on the aluminum surface [12]. From Fig. 3 (c, d, and e), the compact PAPs structure with individual spherical particles having different diameter depending on the polymers can be observed. Compared with PmAP (d) and PpAP (e) films, PoAP film (c) has relatively larger grain and less compact structure.

Characteristics of platinum nano-particles deposited PAPs films

Electrochemical deposition of platinum onto PAPs films was accomplished either by potentiostatic and potentiodynamic methods as described in "Experimental" section. In the potentiostatic experiments, integration of the current was carried out to determine the loading level of platinum in the films. Figure 4 shows the cyclic voltammograms of Al/Pt/PAPs/Pt in potential range −0.40 to 1.0 V in 0.1 M sulfuric acid electrolyte. As can be seen in Fig. 4a, after deposition of Pt in the polymer film, the cyclic voltammogram of modified electrode shows that excessive couple peaks, *a* and *b* (compared with CV grams of Al/Pt/P*o*AP), appeared in positive potentials region corresponding to the formation of platinum oxide and its stripping at the reverse scan. A closer examination of the CV profile in potential range −0.4 to 0.1 V in Figs. 2a and Fig. 4a shows that the shape of CV profile in Fig. 4a is similar to that of Fig. 2a in electrolyte solutions. On the other hand, there are no well-defined peaks corresponding to the adsorption/desorption of hydrogen on platinum, which confirms that a good dispersion of platinum nano-particles in the P*o*AP film is

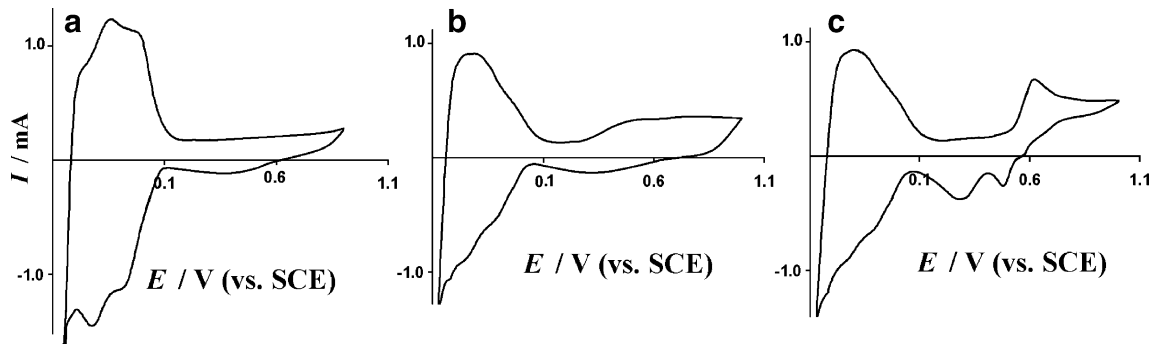

Fig. 2 Cyclic voltammograms of Al/Pt/PAPs electrodes in 0.1 M sulfuric acid electrolyte solution at a scan rate of 50 mV s^{-1} in the absence of monomers. **a** Al/Pt/P*o*AP, **b** Al/Pt/P*m*AP, and **c** Al/Pt/P*p*AP. Amount of Pt on the Al, 6 μg cm^{-2}; polymers film thickness, 0.6 μm

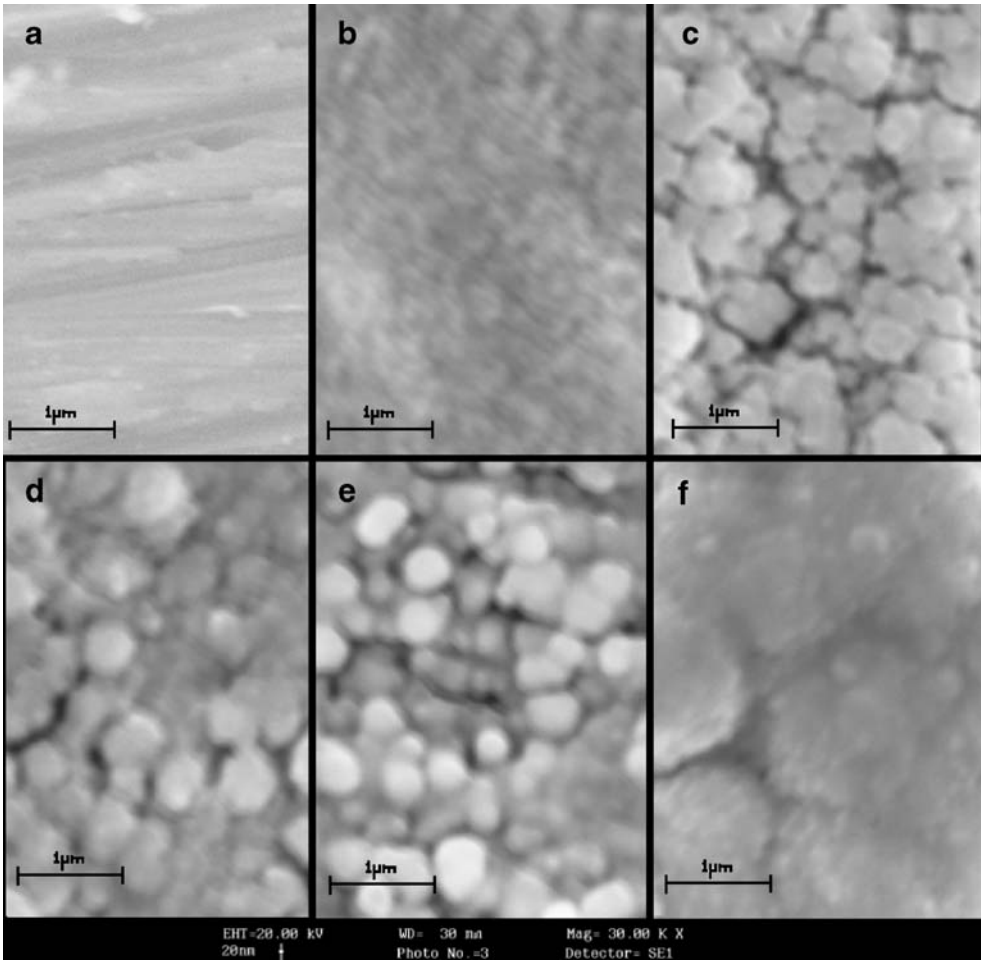

Fig. 3 SEM images of Al electrode surface immediately after polishing (**a**), pre-treated Al (Al/Pt) (**b**), Al/Pt/P*o*AP (**c**), Al//Pt/P*m*AP (**d**), Al//Pt/P*p*AP (**e**), and Al/Pt/P*o*AP/Pt (**f**). Amount of Pt on the Al, 6 μg cm^{-2}; polymers film thickness, 0.6 μm; and amount of Pt loading onto polymers, 0.2 mg cm^{-2}

achieved. Because, if there are platinum islands like the bulk platinum electrode, the hydrogen adsorption/desorption properties of Al/Pt/P*o*AP electrode should have appeared [57]. Similarly, Fig. 4b and c shows the cyclic voltammograms of Al/Pt/P*m*AP/Pt and Al/Pt/P*p*AP/Pt electrodes. As can be seen in these figures, the cyclic voltammograms of Al/Pt/P*m*AP/Pt and Al/Pt/P*p*AP/Pt have only slight differences with respect to CV gram of Al/Pt/P*o*AP/Pt in the electrolyte solution.

As a typical example, Fig. 3f shows the morphology of the Al/Pt/PoAP after deposition of 0.2 mg cm^{-2} of Pt by potentiostatic method. As seen in this image, the large spherical aggregates even 2 μm in diameter may be formed through the settlement of several small nano-particles of Pt. Thus, the distance between settled particles is the behavior responsible for the effective surface are of the aggregate. The images obtained for larger Pt amounts (not illustrated) showed that the aggregates are superposed; this means that

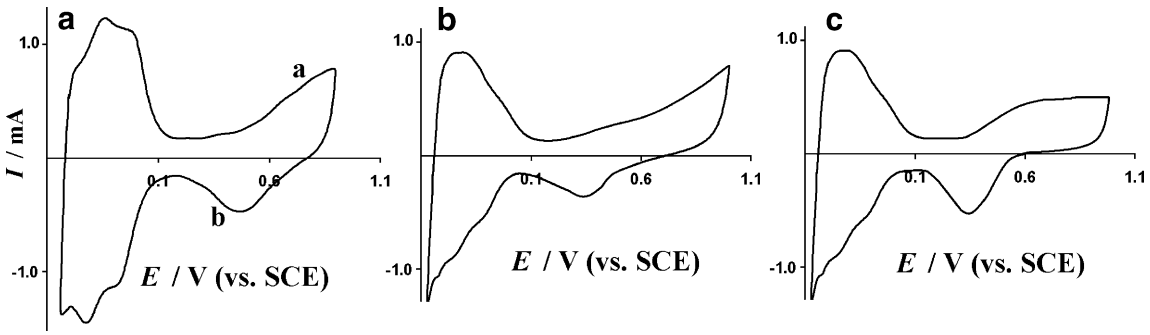

Fig. 4 Cyclic voltammograms of Al/Pt/PAPs/Pt electrodes in 0.1 M sulfuric acid electrolyte solution at a scan rate of 50 mV s^{-1}. **a** Al/Pt/P*o*AP/Pt, **b** Al/Pt/P*m*AP/Pt, and **c** Al/Pt/P*p*AP/Pt. Amount of Pt on the Al, thickness of polymers, and amount of Pt loading as in Fig. 3

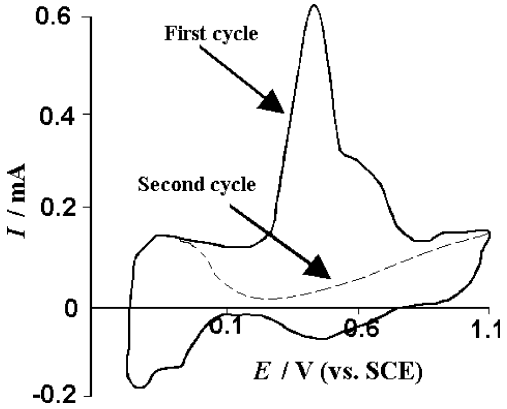

Fig. 5 Cyclic voltammograms of adsorbed CO on the Al/Pt/P*o*AP/Pt electrode in 0.1 M sulfuric acid at 25 °C with scan rate of 5 mV s^{-1} (first and second sweeps). Amount of Pt on the Al, thickness of polymer, and amount of Pt loading as in Fig. 3

the increase of the Pt amount does not contribute to an effective increase in the area.

The real surface area, A_r, of the Pt dispersed electrode was estimated either from the hydrogen adsorption/desorption region in a cyclic voltammograms recorded on the Pt electrocatalyst under a nitrogen atmosphere or from the quantity of electricity for the oxidation of a monolayer of pre-adsorbed CO [58]. As can be seen in Fig. 4, for these composite electrodes, the hydrogen adsorption/desorption region is not visible; therefore, the true surface area was determined from the electrooxidation of a monolayer of adsorbed carbon monoxide [7, 59, 60], assuming that the oxidation of a full CO monolayer involves 420 μC cm^{-2} [59]. The first voltammetric sweep recorded for the composite electrodes after CO adsorption displays, besides the redox peaks of composite electrode, CO oxidation peak (example of such cyclic voltammograms is given in Fig. 5 for Al/Pt/P*o*AP/Pt). The second sweep, recorded under nitrogen atmosphere, only displays the usual redox peaks of composite electrodes, showing that the adsorbed CO layer was completely oxidized (Fig. 5, dashed line). From difference between voltammograms recorded without and with adsorbed CO, the quantity of electricity for CO oxidation was calculated, and hence, an approximate value of the true surface area was obtained.

The surface area of the different investigated electrodes, together with other physical characteristics, was evaluated and given in Table 1. Considering that all composite electrodes have a geometric surface area equal to 0.07 cm^2, the normalized active area (divided by 0.07) of the Al/Pt/P*o*AP/Pt electrode is 18%, and 36% higher than those of Al/Pt/P*m*AP/Pt and Al/Pt/P*p*AP/Pt electrodes, respectively.

Note that the real surface area of Pt-loaded Al electrode (0.2 mg cm^{-2} of Al surface) denoted in the present work with Al–Pt as a comparative electrocatalyst was determined from the quantity of electricity associated with the hydrogen adsorption/desorption region assuming 210 μC cm^{-2} for a full monolayer of adsorbed hydrogen [7].

Electrocatalytic properties of the electrodes toward the electrooxidation of methanol

A primary investigation by cyclic voltammetry showed that methanol did not oxidize on the Al/Pt/PAPs electrodes (e.g., Fig. 6a for the Al/Pt/P*o*AP), but its oxidation is well achieved on the Al/Pt/PAPs/Pt electrodes. In all experiments, the working electrode is submerged in open-circuit position into methanol solution. All cyclic voltammograms are recorded by sweeping the potential from 0.0 to 1.0 V (vs. SCE) and vice versa, without any stay in starting potential. On the basis of the active area values, the real current densities for methanol electrooxidation on electrodes with different polymer films were calculated, and the resulting cyclic voltammograms for Al/Pt/P*o*AP/Pt, Al/Pt/P*m*AP/Pt and Al/Pt/P*p*AP/Pt are shown in Fig. 6b–d. Taking into account the electrode active areas, the Al/Pt/P*o*AP/Pt electrode presents the highest electrocatalytic activity, with current density values almost 20% and 37% higher than those for Al/Pt/P*m*AP/Pt and Al/Pt/P*p*AP/Pt respectively. Additionally, methanol oxidation on Al/Pt/P*o*AP/Pt starts at less positive potentials than two others. Also, there are 40–60 mV potential shifts toward potential

Table 1 Physical characteristics of the different platinum embedded and deposited electrodes

Pt embedded or deposited electrodes	Pt loading W (mg cm^{-2})	True surface area A_r (cm^2)	Specific surface area S (m^2 g^{-1})	Particle size d (nm)
Al/Pt/P*o*AP/Pt	0.2	2.2[a]	15.7	17.9
Al/Pt/P*m*AP/Pt	//	1.7[a]	12.2	23.1
Al/Pt/P*p*AP/Pt	//	1.4[a]	10.0	28.0
Al–Pt	//	0.23 [b]	1.6	170.7
Bulk Pt	Bulk Pt	0.1[b]	–	–

[a] As determined from CO adsorption

[b] As determined from hydrogen adsorption

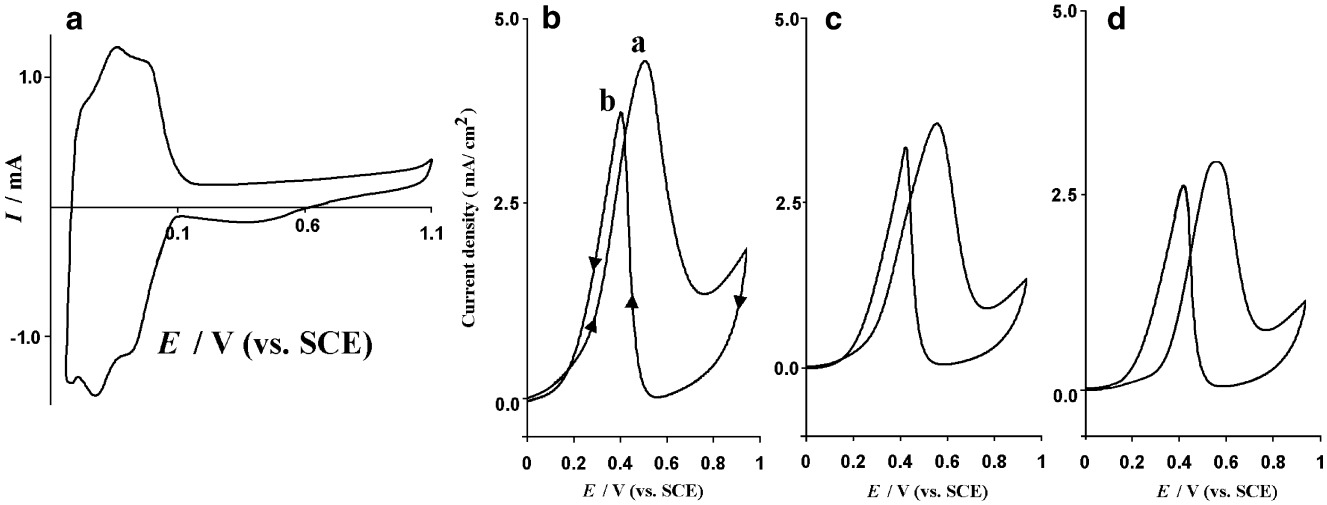

Fig. 6 Cyclic voltammograms of 0.1 M methanol on **a** Al/Pt/P*o*AP, **b** Al/Pt/P*o*AP/Pt, **c** Al/Pt/P*m*AP/Pt, and **d** Al/Pt/P*p*AP/Pt modified electrodes in 0.1 M sulfuric acid at 25 °C with scan rate of 20 mV s^{-1}. Amount of Pt on the Al, thickness of polymers, and amount of Pt loading as in Fig. 3

peak values between the Al/Pt/P*o*AP/Pt electrode and other electrodes showing that the Al/Pt/P*o*AP/Pt electrode is more active for methanol oxidation than the Al/Pt/P*m*AP/Pt and Al/Pt/P*p*AP/Pt electrodes. This observation led us to prefer P*o*AP over two other polymers in construction of the composite electrode.

The crucial effect of PAPs film on the enhancement of platinum nano-particles efficiency toward the electrocatalytic oxidation of methanol is on accordance with our previously reported results [25]. It has been reported that the use of a more porous matrix of conductive polymers allows a better dispersion of electrocatalytic particles through larger portion of the surface and thus prevent agglomeration of metallic particles [61]. Thus, the differences observed between the P*o*AP and others polymers can be attributed, to the more porous, to some extent larger grain and less compact structure of PoAP relative to two others (see Fig. 3c, d, and e), which cause, on one hand, the different active surface area of the dispersed Pt particles with regular, fine distribution and high conductivity of the polymer film and, on the other hand, higher permeability respect to methanol molecules [25].

To further study the effect of P*o*AP film on the enhancement of platinum nano-particle efficiency toward the catalytic oxidation of methanol, the electrocatalytic activity of Pt nano-particle confined Al/Pt/P*o*AP electrode was evaluated and compared with electrocatalytic activity of smooth Pt and Al–Pt electrodes. The cyclic voltammograms in Fig. 7 show the electrooxidation of methanol on (a) Al/Pt/P*o*AP/Pt, (b) Al–Pt of same Pt loading, 0.2 mg cm^{-2}, and (c) smooth Pt electrodes in 0.1 M sulfuric acid + 0.1 M methanol solution, respectively. These results clearly reveal that the Al/Pt/P*o*AP/Pt electrode has significantly greater electrocatalytic activity than the other electrodes.

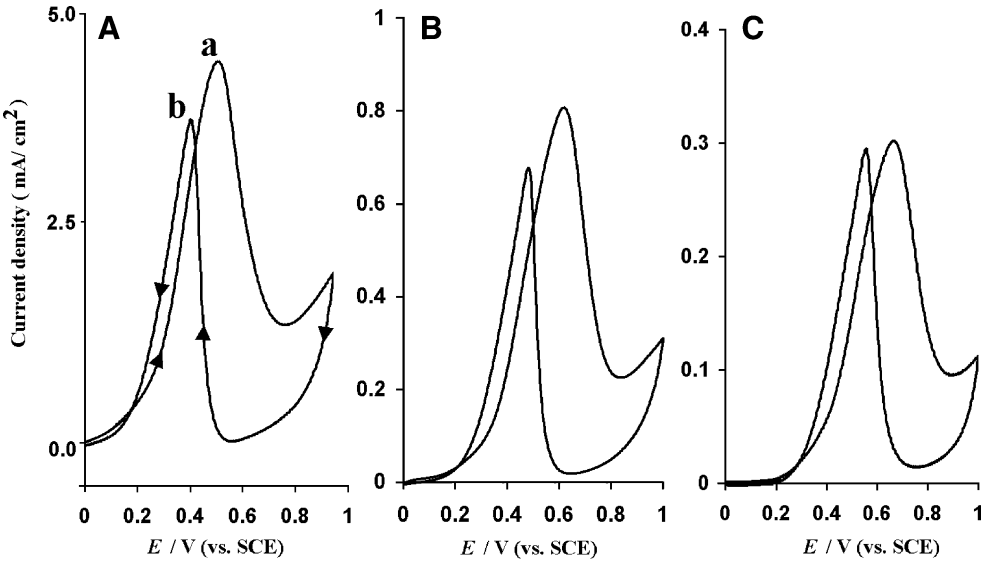

Fig.7 Cyclic voltammograms of 0.1 M methanol on **a** Al/Pt/P*o*AP/Pt electrode, **b** Al–Pt, and **c** smooth Pt electrodes in 0.1 M sulfuric acid at 25 °C with scan rate of 20 mV s^{-1}. Amount of Pt on the Al, thickness of polymer, and amount of Pt loading in polymer film as in Fig. 3; amount of Pt in the Al–Pt, 0.2 mg cm^{-2}

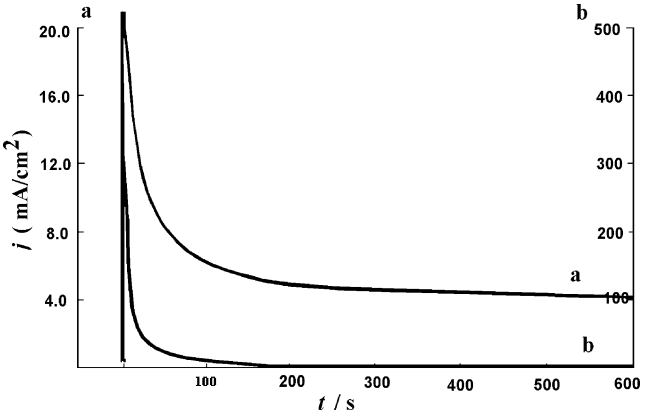

Fig. 8 *j*~*t* transients for methanol oxidation on (*a*) Al/Pt/P*o*AP/Pt and (*b*) a Pt smooth electrodes in 0.1 M sulfuric acid + 0.1 M methanol solution. E_{ox}=0.5 V vs. SCE. Amount of Pt on the Al, thickness of polymer, and amount of Pt loading as in Fig. 3

For example, at the anodic peak, the Al/Pt/P*o*AP/Pt electrode has a current density of about 4.6 mA cm^{-2}, nearly 5.5 times higher than that of the Al–Pt (0.83 mA cm^{-2}) and 15.4 times greater than the smooth Pt electrode. Furthermore, methanol oxidation occurs at much lower oxidation potentials (+506 mV) on the Al/Pt/PoAP/Pt electrode than on the Al–Pt electrode (+617 mV) and smooth Pt electrode (+660 mV).

From Fig. 7a, it can be seen that the current in electrooxidation of methanol on the Al/Pt/P*o*AP/Pt electrode (Pt loading, 0.2 mg cm^{-2}) begins to increase rapidly just above 0.25 V, and an oxidation peak appears at around 0.51 V in the positive going potential sweep (PGPS). This peak is assigned to the oxidation of both reactive intermediates, referred to the direct oxidation of methanol, and the poisoning species derived from methanol dissociative adsorption. In the negative going potential sweep (NGPS), an oxidation current peak attributed to the direct oxidation of methanol emerges at about 0.40 V, right after a small reduction peak appearing at 0.55 V. It is worth mentioning that the peak potential of methanol oxidation in the PGPS shifts negatively by about 0.10 V as compared to the other electrodes, indicating that the Al/Pt/P*o*AP/Pt electrode exhibits high electrocatalytic activity for methanol oxidation. The description of the oxidation peak and the possible mechanism are interpreted in detail elsewhere [4, 57, 62, 63], which emphasized the effect of the diversified Pt oxide on the characteristic of the methanol oxidation.

Obviously, the enhanced catalytic activity of Al/Pt/P*o*AP/Pt electrode for methanol oxidation arises from the existence of Pt nano-particles distributed in P*o*AP matrix. We hypothesize two main reasons for enhanced electrocatalytic activity toward methanol oxidation of the Al/Pt/P*o*AP/Pt electrode compared with the other electrodes [62, 64, 65]: (1) the crystalline size of the Pt particles via a change in the structure of the platinum deposits as a decrease of the average particle size and an increase of the specific surface of electrodes and the fact that platinum nano-particles are less sensitive to the poisoning effect of strongly adsorbed species and (2) the distribution of the Pt nano-particles in the matrix. A high surface area of Pt nano-particles is anticipated due to the uniform distribution of Pt nano-particles in the three-dimensional P*o*AP network (see Table 1). Moreover, the presence of P*o*AP film as a grafted chain electrostatically stabilizes the Pt nano-particles and prevents aggregation of nano-particles. As a result, smaller nano-particles of Pt can be well distributed in the P*o*AP matrix. In addition, the result obtained from the programmed potential step studies is in agreement with the CVs results. Figure 8 shows the comparison of *j*~*t* curves for methanol oxidation on the Al/Pt/P*o*AP/Pt electrode (curve *a*) and on the Pt polycrystalline electrode (curve *b*) at 0.50 V. It can be seen that the methanol oxidation real current density (based on true surface area bulk Pt, A_r, 0.1 cm^2) on Pt polycrystalline electrode decays rapidly with the time, and the current density in *j*~*t* curve almost reached zero after 500 s. The rapid current density decay has been interpreted as the "self-poisoning" of the adsorbed species derived from the dissociative adsorption of methanol [66]. Correspondingly, the real current density of methanol oxidation on Al/Pt/P*o*AP/Pt electrode decreases comparatively slowly. When the time is above 500 s, the current density reaches a relatively stable value, which is still about one fifth of the initial current. It is obvious that the Al/Pt/P*o*AP/Pt electrode exhibits a higher electrocatalytic activity and stability toward methanol oxidation. Similar results have been reported (see Table 2) for deposition of some catalyst at bare and composite electrodes [20, 22, 25, 60, 67–82]. It has been suggested that the polymeric structures prevent the nano-particles from agglomerating and coalescing during deposition and also stabilize them on the electrode. A three-dimensional growth of deposited nano-particles in the presence of polymeric films instead of a two-dimensional growth at bare electrodes is also postulated [68]. Thus, the role of the polymeric matrix is not connected with an increase of the intrinsic specific activity of electrocatalysts. Indeed, the films are good and proper bed for deposition of electrocatalyst particles and increase the electrocatalysis active sites; ultimately, the anodic current for the oxidation of methanol is increased.

In order to reveal the correlation between methanol oxidation and Pt oxide species, we have studied the effect of upper limit potentials (EU) in cyclic potential scanning on the methanol oxidation. Figure 9 shows the cyclic voltammograms of methanol oxidation on the Al/Pt/P*o*AP/Pt electrode for EU of 0.6 to 1.30 V. As seen in Fig. 9 by increasing the final positive potential limit, the anodic

Table 2 Effect of conductive polymer supports on the catalytic activity of Pt particles in methanol oxidation

No.	Composite electrode (CE)	Bulk or Pt particles on bare substrate (BE)	Ratio of real current density[a] (CE/BE)	Ref.
1	C/PANI/Pt	C/Pt	3.3	77
2	GC/PANI/Pt	Pt/Pt	3.6	79
3	ITO/PEDOT-PSS-Pt	Pt	5.5	83
4	SS/PANI/Pt	SS/Pt	1.5	74
5	GC/SBA-15/Pt	GC/Pt	>>1	72
6	GC/PAANI/Pt	GC/Pt	2.5	75
7	GC/PDDA/Pt	GC/Pt	2.1	71
8	ITO/PEDOT-PSS/H_xMoO_3-Pt	ITO/H_xMoO_3-Pt	1.4	82
9	Al/Pt/PoAP/Pt	Al/Pt	5.5	This work

[a] Current density per real surface area of Pt particles

current of methanol oxidation in the PGPS remains unchanged, but oxidation current in the NGPS is decreased. In lower limit potential, the Pt oxides with high valence have not developed greatly, so the effect of the Pt oxides with high valence on methanol oxidation in the NGPS is relatively small. It can be seen that the potential of methanol oxidation peak remains invariable in the PGPS, while the potential of methanol oxidation peak shifts positively in the NGPS. On the other hand, the peak current in the NGPS decreased as the EU increased. Indeed, by increasing final positive potentials, the conversion of Pt to PtO is accelerated and caused a decrease of oxidation current in the NGPS, which further demonstrates that methanol can only be oxidized on clean metallic platinum nano-particles surface [13, 83].

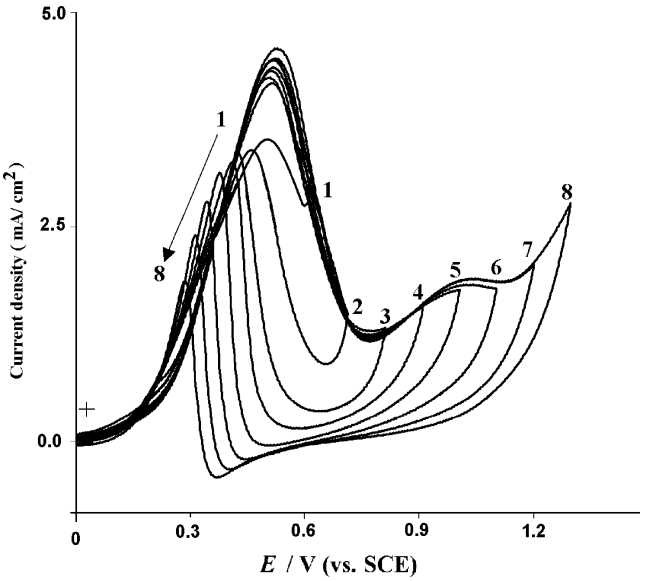

Fig. 9 Effect of upper limit of potential scanning region on the electrooxidation of 0.1 M methanol in 0.1 M sulfuric acid on the Al/Pt/PoAP/Pt electrode. (*1*) 0.0 to 0.6 V, (*2*) 0.0 to 0.7 V, (*3*) 0.0 to 0.8 V, (*4*) 0.0 to 0.9 V, (*5*) 0.0 to 1.0 V, (*6*) 0.0 to 1.1 V, (*7*) 0.0 to 1.2 V, (*8*) 0.0 to 1.3 V. Scan rate of 20 mV s^{-1}. Amount of Pt on the Al, thickness of polymer, and amount of Pt loading as in Fig. 3

Parameters affecting the electrocatalytic behavior of composite electrode

As noted in the literatures, a strong dependence of the platinum metal catalytic activity on the catalyst particle structure, its distribution within matrix of conducting polymers, etc. are marked for the electrooxidation reaction of methanol. It is desirable that the adjustment of the parameters would allow the electrocatalytic nature of the composite electrode to be optimized.

Effect of PoAP film thickness

Electropolymerization offers the possibility of controlling the thickness and homogeneity of the conducting polymer film at the electrode surface. Electropolymerization of *o*-aminophenol on pre-treated Al disk was done by potentiodynamic method in the potential limits from −0.4 to 1.0 V at a sweep rate of 50 mV s^{-1} in a solution containing 80 mM *o*AP and 0.1 M sulfuric acid. To study the effect of P*o*AP films thickness on the electrodeposition of platinum nano-particles and the subsequent electrocatalytic activity for methanol oxidation, a series of experiments are performed to electropolymerize the P*o*AP films on the Al/Pt disk in the same solutions and with the same potential limits and sweep rates, while the cycle numbers are altered to 30, 40, 60, 70, and 80, respectively. By observing the feature of the electrode surface, it is found that corresponding to the cycle numbers of 30–80, the color of the P*o*AP films changes gradually from redwhish to red. Thickness of the P*o*AP films formed with the above-mentioned cycle numbers corresponds to 0.1–1.2 μm. After the P*o*AP films are formed individually, platinum nano-particles are electrodeposited, respectively, by potentiostatic method, and the oxidation of methanol is investigated with

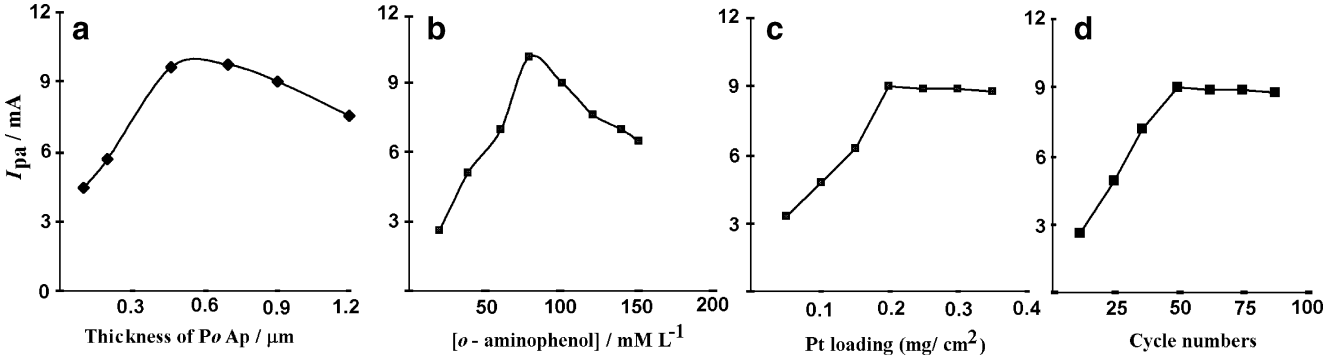

Fig. 10 Plot of anodic peak current of 0.1 M methanol in 0.1 M sulfuric acid solution for Al/Pt/P*o*AP/Pt electrode as a function of **a** thickness of polymer, **b** monomer concentration, **c** platinum loading in potentiostatic method, and **d** cycle numbers of platinum loading in potentiodynamic method. Amount of Pt on the Al, thickness of polymer, and amount of Pt loading as in Fig. 3

these platinum-incorporated P*o*AP electrodes. Figure 10a shows the effect of thickness of P*o*AP films modified with same amount of platinum nano-particles (0.2 mg cm^{-2}) on the oxidation peak current of methanol. As is seen, the anodic current rises progressively for the film thickness up to 0.5 μm and remains constant to 0.7 μm and drops afterward. This implies that the electrocatalysis of methanol oxidation is sensitive to thickness of the polymer film. The increase in the peak current for the thickness of polymers up to 0.5 μm may be attributed to the occupation of Pt nano-particles in the pores of polymers with the real sizes. Thicknesses from 0.5 to 0.7 μm have the optimum structure and porosity for incorporation of Pt. The decrease beyond 0.7 μm may be due to the lessening of real surface area of Pt nano-particles by the excessive presence of polymers on the surface of the electrode. In the following experiments, therefore, the P*o*AP films being electropolymerized by 50 cycles (0.6 μm thickness) are used as the matrix to electrodeposit platinum nano-particles.

Effect of monomer concentration

The influence of monomer concentration during the electrosynthesis of P*o*AP film with certain thickness on the reactivity of the composite electrodes was investigated by varying the concentration of *o*-aminophenol from 20 to 150 mM. In these experiments, the charge corresponding to the polymer formation films was 140 mC cm^{-2}. The results obtained (Fig. 10b) for the peak currents related to the electrooxidation of methanol in these conditions show that there is an increase in the electrooxidation peak current of methanol when there is an increase in the monomers concentration from 20 to about 80 mM. A current decrease can be observed when the higher monomer concentrations are used. This may be attributed in one hand to the lower conductivity and poor electroactivity of thick film and in other hand to the simultaneous formation of some oligomers during electropolymerization of *o*-aminophenol of high concentration. Thus, the formation of the oligomers affects the morphology of the polymer film, which decreases the amount of platinum nano-particles dispersed in the film and effective surface area of the Pt and influences the poisoning extent of the dispersed platinum nano-particles via the adsorption of some methanol oxidation intermediates.

Effect of platinum loading procedure and platinum amount

Potentiostatic method

The effect of the platinum deposition potentials on the electrooxidation of methanol was tested by recording the corresponding cyclic voltammogram after each deposition process, in solution containing 0.1 M methanol and 0.1 M sulfuric acid solution as supporting electrolyte. The results show that the peak current for electrooxidation of methanol increases when the deposition potential is changed from −0.4 up to −0.1 V. The oxidation peak current observed was greater as the loading potential was less negative and level off at about −0.2 V. Referring to some reports, this was attributed to the slower electrodeposition of Pt that generates a higher Pt surface due to the formation of small nano-particles [23, 57, 65]. This explanation seems to be unreasonable as we know less that negative potential in reduction process has smaller drive force to promote nucleation and will be advantageous for the growth and formation of large particles. Therefore, the observed results in agreement with those reported in the literature may be explained by considering the other phenomena governing the electrodeposition of the platinum nano-particles. Indeed, at more negative potential, there are two possible parallel reactions: (1) reduction of Pt^{4+} to metallic platinum and (2) hydrogen evolution on the electrodeposited platinum nano-particles; therefore, the Pt nano-particles obtained show irregular shapes, and thus, Pt deposition is not uniform [84].

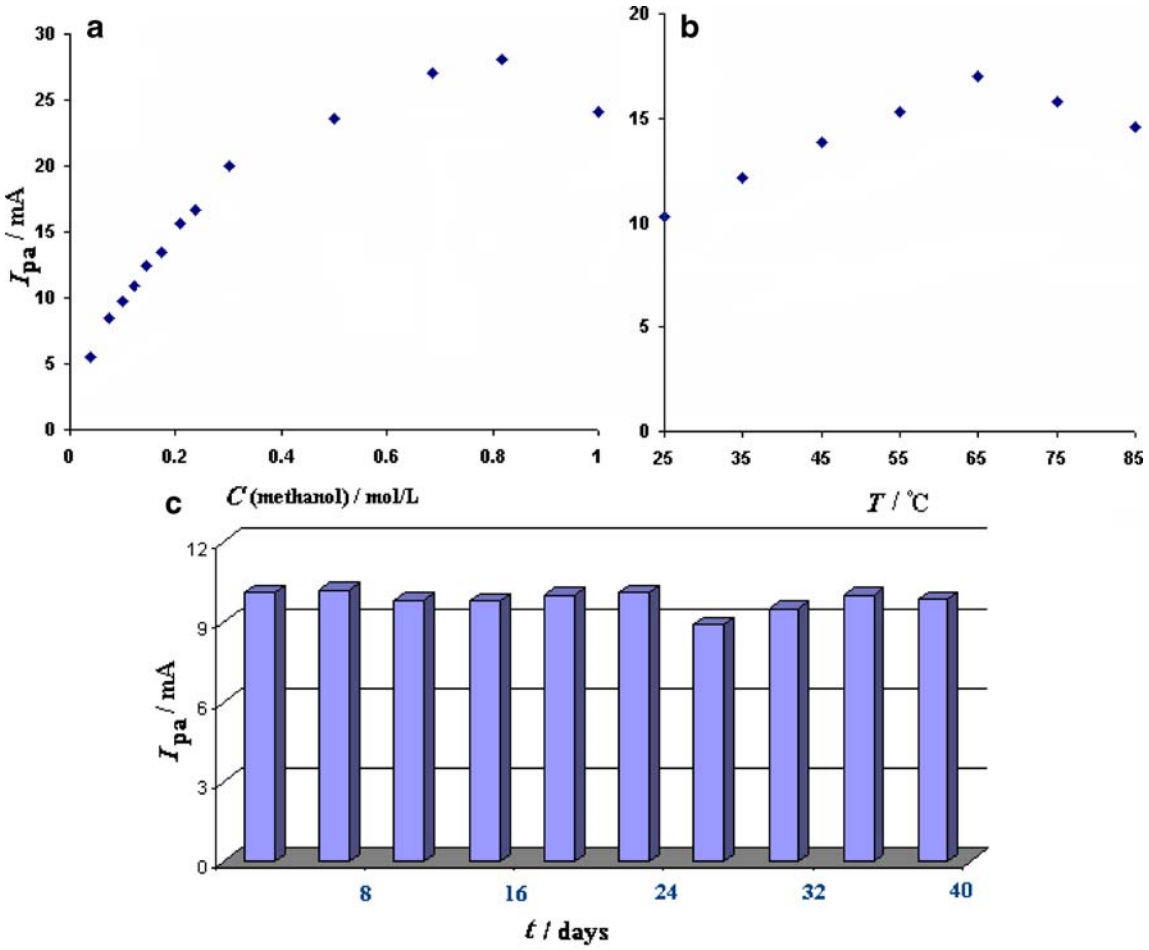

Fig. 11 Plot of anodic peak current of methanol oxidation on the Al/Pt/P*o*AP/Pt electrode in 0.1 M sulfuric acid solution as a function of methanol concentration (**a**). Plot of anodic peak current of 0.1 M methanol as a function of medium temperature (**b**) and time (**c**). Amount of Pt on the Al, thickness of polymer, and amount of Pt loading as in Fig. 3

It is obvious that the anodic current of methanol oxidation depends on the amount of Pt incorporated in the film. The variation of the anodic peak currents, which appear in the PGPS as a function of Pt loading, are shown in Fig. 10c (at electrodes with the same thicknesses of polymer films). As is seen in Fig. 10c, I_{pa} increases with increasing amount of the Pt incorporated in the each polymer films and level off at 0.2 mg cm^{-2}. Indeed, thereafter, any extra platinum loading does not increase the catalytic activity of the electrodes, probably because of a constant active surface area.

Potentidynamic method

In this procedure for preparation of platinum-modified P*o*AP electrode with different platinum loadings, the platinum nano-particles are electrodeposited into P*o*AP films (0.6 μm) by cyclic voltammetry in same potential range and same scan rate, but with various cycle numbers. As expected, the platinum loadings will be increased successively with increasing cycle numbers of platinum electrodeposition. The amount of Pt particles loaded onto the Al/Pt/PoAP was also calculated from Eq. 1. In this case, the charge (Q_{dep}), which utilized for the deposition of Pt particles, was obtained through graphical integration of cyclic voltammetric curves [81].

Cyclic voltammograms of methanol oxidation on the Al/Pt/P*o*AP/Pt composite electrodes with different platinum loading show that the methanol oxidation begins to increase rapidly just above 0.25 V, and with varying amount of platinum particles deposited, the shift of potentials of the current peak is not obvious. Moreover, the variations of the anodic peak currents, which appear in the PGPS as a function of cycle numbers of platinum electrodeposition, are well pronounced (Fig. 10d). It means that up to the largest cycle numbers (50 times) of platinum electrodeposition in this experiment, the platinum atoms can form small clusters inside the P*o*AP film, and these clusters appear to be sufficiently dispersed in the overall structure of the P*o*AP film. In other words, no “platinum island”

resembled a bulk platinum electrode in property forms. Beyond this, any extra platinum loading by increasing the cyclic numbers does not increase the catalytic activity of the electrode. The effect of scan rate and potential limits with constant cycle numbers in hydrodynamic method on the anodic peak current of methanol oxidation was also examined, and optimum conditions 50 mV s^{-1} and −0.3 to 0.8 V were obtained, respectively, for sweep rate and potential limits.

It is worth mentioning that the platinum loading method has little effect on the anodic current of methanol oxidation (see Fig. 10c and d).

Effect of methanol concentration

Figure 11a shows the effect of methanol concentration on the anodic current of methanol oxidation at Al/Pt/P*o*AP/Pt electrode. It is clearly observed that the anodic current increases with increasing methanol concentration and levels off at concentrations higher than 0.8 M. We assume that this effect may due to the saturation of active sites on the surface of the electrode. In accordance with this result, the optimum concentration of methanol to obtain a higher current density may be considered as about 0.8 M.

Effect of medium temperature and stability of the electrode responses

The effect of medium temperature on the anodic current is shown in Fig. 11b. A linear increase in the peak current with increasing temperature is observed up to 65 °C, indicating an enhancement of the methanol oxidation rate with temperature. The next decrease of peak current can be attributed to the progressive evaporation of methanol with rising the temperature. Assuming that no azeotrope is formed in methanol water mixture, it is expected that a progressive decrease in peak current should appear during the temperature elevation because of a loss in methanol concentrations. However, a linear increase of the peak current is observed in practice at temperatures below 65 °C (the boiling point of methanol is 64.5 °C), which can be assigned to the acceleration of the electrode reaction kinetics proportionally to temperature increase. Accordingly, on the basis of the above results, an optimum temperature of 60 °C is proposed for methanol electrooxidation on the Al/Pt/P*o*AP/Pt electrode (in 0.1 M methanol + 0.1 M sulfuric acid solution).

Figure 11c shows the responses of electrode stored in laboratory atmosphere and in the course of time. The results indicate that the responses are reproducible up to 40 days, which is indicative of the nearly long-term stability of P*o*AP modified electrode.

Note that the similar results were obtained by Al/Pt/P*m*AP/Pt and Al/Pt/P*p*AP/Pt electrodes.

Conclusion

The Al/Pt electrode modified by thin film of poly (aminophenols) incorporating platinum nano-particles exhibit the electrocatalyst activity toward the methanol oxidation. The results show that modification of pre-treated electrode surface by P*o*AP improves the electrocatalytic activity for methanol oxidation to a great extent. When the value of Pt loading is 0.2 mg cm^{-2}, the Al/Pt/P*o*AP/Pt electrode is greatly superior to the Al–Pt of the same Pt loading and smooth Pt electrodes in electrocatalytic activity. Factors such as thickness of polymer, monomer concentration, Pt loading, methanol concentration, and medium temperature all influence the anodic current of methanol electrooxidation on the Al/Pt/P*o*AP/Pt electrode significantly. These preliminary results show that the composite electrode proposed is very effective for methanol oxidation, but the electrode systems aimed to apply in fuel cells, and further studies are necessary to address the above issues and that as such the paper is a “work in progress”.

References

1. Janssen MMP, Moolhuysen J (1977) J Catal 46:289. doi:10.1016/0021-9517(77) 90212-3
2. Parsons R, VanderNoot T (1988) J Electroanal Chem 257:9. doi:10.1016/0022-0728(88) 87028-1
3. Ross PN (1991) Electrochim Acta 36:2053. doi:10.1016/0013-4686(91) 85209-P
4. Iwasita T (2002) Electrochim Acta 47:3663. doi:10.1016/S0013-4686(02) 00336-5
5. Liu H, Song C, Zhang L, Zhang J, Wang H, Wilkinson DP (2006) J Power Sources 155:95
6. Habibi B, Pournaghi-Azar MH, Razmi H, Abdolmohammad-Zadeh H (2008) Int J Hydrogen Energy 33:2668. doi:10.1016/j.ijhydene.2008.03.014
7. Gloaguen F, Leger J-M, Lamy C (1997) J Appl Electrochem 27:1052. doi:10.1023/A:1018434609543
8. Mahe E, Devilliers D, Groult H, Pouilleau J (1999) Electrochim Acta 44:2307. doi:10.1016/S0013-4686(98) 00352-1
9. Stoychev D, Papoutsis A, Kelaidopoulou A, Kokkinidis G, Milchev A (2001) Mater Chem Phys 72:360. doi:10.1016/S0254-0584(01) 00337-6
10. Hao Yu E, Scott K, Reeve RW, Yang L, Allen RG (2004) Electrochim Acta 49:2443. doi:10.1016/j.electacta.2004.01.022
11. Gojkovic SL (2004) J Electroanal Chem 573:271. doi:10.1016/j.jelechem.2004.07.013
12. Pournaghi-Azar MH, Habibi-A B (2005) J Electroanal Chem 580:23. doi:10.1016/j.jelechem.2005.02.021
13. Nozad AG, Ghannadi MM, Sedaghat SS, Taghi-Ganji KM, Yari M (2006) Electroanalysis 18:911. doi:10.1002/elan.200503476
14. Hamnett A, Kennedy BJ (1988) Electrochim Acta 33:1613. doi:10.1016/0013-4686(88) 80233-0

15. Hable TC, Wrighton MS (1991) Langmuir 7:1305. doi:10.1021/la00055a001
16. Gurau B, Viswanathan R, Liu R, Lafrenz TJ, Reddington E, Sapienza A, Chan BC, Mallouk TE, Sarangapani S (1998) J Phys Chem B 102:9997. doi:10.1021/jp982887f
17. Götz M, Wendt H (1998) Electrochim Acta 43:3637. doi:10.1016/S0013-4686(98) 00121-2
18. Ralph TR, Hogarth MP (2002) Platin Met Rev 46:117
19. Malinauskas A (1999) Synth Met 107:75. doi:10.1016/S0379-6779(99) 00170-8
20. Golabi SM, Nozad A (2002) J Electroanal Chem 521:161. doi:10.1016/S0022-0728(02) 00656-3
21. Niu L, Li Q, Wei F, Chen X, Wang H (2003) J Electroanal Chem 544:121. doi:10.1016/S0022-0728(03) 00085-8
22. Rajesh B, Thampi KR, Bonard J-M, McEvoy AJ, Xanthopoulos N, Mathieu HJ, Viswanathan B (2004) J Power Sources 133:155. doi:10.1016/j.jpowsour.2004.02.008
23. Profeti D, Olivi P (2004) Electrochim Acta 49:4979. doi:10.1016/j.electacta.2004.06.013
24. Mascaro LH, Goncalves D, Bulhoes LOS (2004) Thin Solid Films 461:243. doi:10.1016/j.tsf.2004.01.084
25. Pournaghi-Azar MH, Habibi B (2007) J Electroanal Chem 601:53. doi:10.1016/j.jelechem.2006.10.027
26. Pournaghi-Azar MH, Habibi B (2007) J Electroanal Chem 605:136. doi:10.1016/j.jelechem.2007.03.025
27. Santhosh P, Gopalan A, Vasudevan T, Lee K-P (2006) Appl Surf Sci 252:7964. doi:10.1016/j.apsusc.2005.10.002
28. Kelaidopoulou A, Abelidou E, Kokkinidis G (1999) J Appl Electrochem 29:1255. doi:10.1023/A:1003796616083
29. Barbero C (2005) J Electroanal Chem 576:139. doi:10.1016/j.jelechem.2004.10.013
30. Yamada N, Teshima K, Kobayashi N, Hirohashi R (1995) J Electroanal Chem 394:71. doi:10.1016/0022-0728(95) 04003-7
31. Yang H, Bard AJ (1992) J Electroanal Chem 339:423. doi:10.1016/0022-0728(92) 80466-H
32. Lapuente R, Cases F, Garces P, Morallon E, Vazquez JL (1998) J Electroanal Chem 451:163. doi:10.1016/S0022-0728(98) 00098-9
33. Lofrano RCZ, Madurro JM, Abrantes LM, Romero JR (2004) J Mol Catal Chem 218:73. doi:10.1016/j.molcata.2004.04.001
34. de Castro CM, Vieira SN, Goncalves RA, Brito-Madurro AG, Madurro JM (2008) J Mater Sci 43:475. doi:10.1007/s10853-007-1880-7
35. Li J, Lin X (2007) Biosens Bioelectron 22:2898. doi:10.1016/j.bios.2006.12.004
36. Yuqing M, Jianrong C, Xiaohua W (2004) Trends Biotechnol 22:227. doi:10.1016/j.tibtech.2004.03.004
37. Franco DL, Afonso AS, Vieira SN, Ferreira LF, Gonçalves RA, Brito-Madurro AG, Madurro JM (2008) Mater Chem Phys 107:404. doi:10.1016/j.matchemphys.2007.08.006
38. Hür E, Bereket G, Duran B, Özdemir D, Şahin Y (2007) Prog Org Coat 60:153. doi:10.1016/j.porgcoat.2007.07.026
39. Ortega JM (2000) Thin Solid Films 360:159. doi:10.1016/S0040-6090(99) 00963-3
40. Salavagione HJ, Arias J, Garcés P, Morallón E, Barbero C, Vázques JL (2004) J Electroanal Chem 565:375. doi:10.1016/j.jelechem.2003.11.005
41. Konopelnik OI, Aksimentyeva OI, Grytsiv MY (2002) Mater Sci 20:49
42. Pournaghi-Azar MH, Habibi B (2007) Electrochim Acta 52:4222. doi:10.1016/j.electacta.2006.11.050
43. Pournaghi-Azar MH, Razmi-Nerbin H (1998) J Electroanal Chem 456:83. doi:10.1016/S0022-0728(98) 00284-8
44. McCrone WC, Whitney GF, Corvin I (1949) Anal Chem 21:531. doi:10.1021/ac60028a004
45. Hammachc H, Makhloufi L, Saidani B (2001) Synth Met 123:515. doi:10.1016/S0379-6779(01) 00345-9
46. Pournaghi-Azar MH, Habibi B (2007) J Solid State Electrochem 11:505. doi:10.1007/s10008-006-0187-y
47. Barbero C, Zerbino J, Sereno L, Posadas D (1987) Electrochim Acta 32:693. doi:10.1016/0013-4686(87) 87063-9
48. Hand RL, Nelson RF (1978) J Electrochem Soc 125:1059. doi:10.1149/1.2131621
49. Zhang AQ, Cui CQ, Chen YZ, Lee JY (1994) J Electroanal Chem 373:115. doi:10.1016/0022-0728(94) 03329-3
50. Tucceri RI, Barbero C, Silber JJ, Sereno L, Posadas D (1997) Electrochim Acta 42:919. doi:10.1016/S0013-4686(96) 00277-0
51. Guenbour A, Kacemi A, Benbachir A, Aries L (2000) Prog Org Coat 38:121. doi:10.1016/S0300-9440(00) 00085-0
52. You-Yu Z, Mei-Ling W, Mei-Ling L, Qin Y, Qing-Ji X, Shou-Zhuo Y (2007) Chin. J Anal Chem 35:685
53. Herna'ndez N, Ortega JM, Choy M, Ortiz R (2001) J Electroanal Chem 515:123. doi:10.1016/S0022-0728(01) 00619-2
54. Osaka T, Moma T, Shiota S, Nakamura S (1993) Denki Kagaku 61:136
55. Ortega JM (2000) Thin Solid Films 371:28. doi:10.1016/S0040-6090(00) 00980-9
56. Ohsaka T, Kunimura S, Oyama N (1988) Electrochim Acta 33:639. doi:10.1016/0013-4686(88) 80062-8
57. Niu L, Li Q, Wei F, Wu S, Liu P, Cao X (2005) J Electroanal Chem 578:331. doi:10.1016/j.jelechem.2005.01.014
58. Trasatti S, Petrii OA (1992) J Electroanal Chem 327:353. doi:10.1016/0022-0728(92) 80162-W
59. Croissant MJ, Napporn WT, Le'ger J-M, Lamy C (1998) Electrochim Acta 43:2447. doi:10.1016/S0013-4686(97) 10157-8
60. Venancio EC, Napporn WT, Motheo AJ (2002) Electrochim Acta 47:1495. doi:10.1016/S0013-4686(01) 00877-5
61. Kulesza PJ, Matczak M, Wolkiewicz A, Grzybowska B, Galkowski M, Malik MA, Wieckowski A (1999) Electrochim Acta 44:2131. doi:10.1016/S0013-4686(98) 00321-1
62. Galal A, Atta NF, Darwish SA, Ali SM (2008) Top Catal 47:73. doi:10.1007/s11244-007-9035-2
63. Wasmus S, Küver A (1999) J Electroanal Chem 461:14. doi:10.1016/S0022-0728(98) 00197-1
64. Laborde H, Leger JM, Lamy C (1994) J Appl Electrochem 24:219
65. Becerik İ, Süzer Ş, Kadirgan F (2001) J Electroanal Chem 502:118. doi:10.1016/S0022-0728(00) 00541-6
66. Sun SG, Lipkowski J, Altounian Z (1990) J Electrochem Soc 137:2443. doi:10.1149/1.2086958
67. Golabi SM, Nozad A (2003) Electroanalysis 15:278. doi:10.1002/elan.200390035
68. Weisshaar DE, Kuwana T (1984) J Electroanal Chem 163:395. doi:10.1016/S0022-0728(84) 80067-4
69. Cai LT, Chen HY (1998) J Appl Electrochem 28:161. doi:10.1023/A:1003226624506
70. Bouzek K, Mangold K-M, Jüttner K (2001) J Appl Electrochem 31:501. doi:10.1023/A:1017527114207
71. Jiang SP, Liu Z, Tang HL, Pan M (2006) Electrochim Acta 51:5721. doi:10.1016/j.electacta.2006.03.006
72. Chen Z-F, Jiang Y-X, Wang Y, Xu J-M, Jin L-Y, Sun S-G (2005) J Solid State Electrochem 9:363. doi:10.1007/s10008-005-0653-y
73. Golikand AN, Golabi SM, Maragheh MG, Irannejad L (2005) J Power Sources 145:116. doi:10.1016/j.jpowsour.2005.02.061
74. Liu F-J, Huang L-M, Wen T-C, Yin K-C, Hung J-S, Gopalan A (2007) Poly Compos 28:650. doi:10.1002/pc.20321
75. Jiang C, Lin X (2007) J Power Sources 164:49. doi:10.1016/j.jpowsour.2006.10.057
76. Selvaraj V, Alagar M, Hamerton I (2006) J Power Sources 160:940. doi:10.1016/j.jpowsour.2006.02.055
77. Kitani A, Akashi T, Sugimoto K, Ito S (2001) Synth Met 121:1301. doi:10.1016/S0379-6779(00) 01522-8
78. Wu G, Li L, Li J-H, Xu B-Q (2005) Carbon 43:2579. doi:10.1016/j.carbon.2005.05.011

79. Mikhaylova AA, Molodkina EB, Khazova OA, Bagotzky VS (2001) J Electroanal Chem 509:119. doi:10.1016/S0022-0728(01) 00479-X
80. Maiyalagan T (2008) J Power Sources 179:443. doi:10.1016/j.jpowsour.2008.01.048
81. Kuo C-W, Huang L-M, Wen T-C, Gopalan A (2006) J Power Sources 160:65. doi:10.1016/j.jpowsour.2006.01.100
82. Kuo C-W, Sivakumar C, Wen T-C (2008) J Power Sources 185:807. doi:10.1016/j.jpowsour.2008.07.060
83. Hu C-C, Liu K-Y (1999) Electrochim Acta 44:2727. doi:10.1016/S0013-4686(98) 00400-9
84. Montilla F, Morallón E, Duo I, Comninellis C, Vázquez JL (2003) Electrochim Acta 48:3891. doi:10.1016/S0013-4686(03) 00526-7